Available online at www.sciencedirect.com
ScienceDirect
Trans. Nonferrous Met. Soc. China 26(2016) 1564−1573
Transactions of Nonferrous Metals Society of China
www.tnmsc.cn

Microstructural evolution and phase transformation during partial remelting of in-situ Mg_2Si_p/AM60B composite

Su-qing ZHANG, Ti-jun CHEN, Fa-liang CHENG, Lei-liang LI

State Key laboratory of Advanced Processing and Recycling of Nonferrous Metals, Lanzhou University of Technology, Lanzhou 730050, China

Received 11 June 2015; accepted 15 September 2015

Abstract: The microstructural evolution and phase transformations during partial remelting of in-situ Mg_2Si_p/AM60B composite modified by SiC and Sr were investigated. The results indicate that SiC and Sr are effective for refining primary α-Mg grains and Mg_2Si particles. After being partially remelted, a semisolid microstructure with small and spheroidal primary α-Mg particles can be obtained. The microstructural evolution during partial remelting can be divided into four stages: the initial rapid coarsening, structural separation, spheroidization and final coarsening, which are essentially caused by the phase transformations of $\beta \rightarrow \alpha$, $\alpha+\beta \rightarrow L$ and $\alpha \rightarrow L$, $\alpha \rightarrow L$, and $\alpha \rightarrow L$ and $L \rightarrow \alpha$, respectively. The Mg_2Si particles have not obvious effect on the general microstructural evolution steps, but can slower the evolution progress and change the coarsening mechanism. During partial remelting, Mg_2Si particles first become blunt and then become spheroidal because of melting of their edges and corners, and finally are coarsened owing to Ostwald ripening.

Key words: magnesium alloy; partial remelting; thixoforming; microstructure evolution; phase transformation; in-situ composite

1 Introduction

Magnesium alloys have large potential in the field of automobiles, electronic products, portable tools, sporting goods and aerospace vehicles [1]. However, AM60B alloy, one of the most commonly used aluminum-bearing magnesium alloys, suffers from the challenge in meeting the requirements in many applications. The most promising way to overcome these shortcomings is to fabricate its based composites [2−4]. It is well known that Mg_2Si particles have high melting point, high hardness, low density, high elastic modulus and low thermal expansion coefficient, and are an ideal reinforcement for magnesium-based composites [5−7]. So, it can be expected that adding silicon element into AM60B alloy melt to form in-situ Mg_2Si_p/AM60B composite should be considered as one of the most potential ways to improve the properties of AM60B alloy [6,8,9]. However, the coarsely dendritic primary Mg_2Si phases and the brittle Chinese script eutectic Mg_2Si phases result in relatively poor properties, and cannot be accepted by engineering applications. The previous investigation indicated that Sr element is an effective refiner for Mg_2Si phase and a composite with Mg_2Si particles (20−40 μm) can be obtained [10]. In addition, thixoforming, a relatively new metal forming technology, can enhance room-temperature mechanical properties through reducing porosities and gas pores, compared with the traditional forming technology of pressure casting [11−14]. Therefore, it can be supposed that thixoforming is a good way for the fabrication of Mg_2Si_p/AM60B components with high performance.

Thixoforming has been widely used to produce aluminum alloy products [15−18]. But the investigations on magnesium alloys are obviously laggard to those of aluminum alloys. Therefore, it is necessary to pay more attention to magnesium-based materials. The key procedure of thixoforming is to produce semisolid ingots with small and spheroidal primary particles uniformly suspended in liquid phase. There are several technologies to fabricate this kind of non-dendritic semisolid ingots, such as magnetohydrodynamic stirring, mechanical stirring, chemical grain refining, near liquidus pouring,

Foundation item: Project (G2010CB635106) supported by the National Basic Research Program of China; Project (NCET-10-0023) supported by the Program for New Century Excellent Talents in University of China; Project supported by the Program for Hongliu Outstanding Talents of Lanzhou University of Technology, China

Corresponding author: Ti-jun CHEN; Tel: +86-931-2976573; Fax: +86-931-2976578; E-mail: chentj@lut.cn; zhangsuqing1985@163.com

DOI: 10.1016/S1003-6326(16)64262-0

spray casting and strain-induced melt activation [19−26]. Among them, chemical grain refining process is a relatively simple method because it does not need special treating procedures [14,22,23]. It produces the desired microstructure by adding grain refiner during traditional casting and a following heat treatment in mushy zone. The key of this method is to obtain cast ingots with fine equiaxed grains. The existing investigation indicates that carbon inoculation is an effective grain refining technique for aluminum-bearing magnesium alloys [27]. The microstructural evolution during partial remelting is another key topic of thixoforming because this process has large effect on the resultant semisolid microstructure. However, the studies on composites, especially in-situ composites, are very scarce compared with their corresponding matrix alloys. Only a few papers have involved the as-cast composites, but focused on the morphology change of the reinforcement particles [28]. Nevertheless, the microstructural evolution prior to liquid formation is very important to clarify the formation of final semisolid microstructure. In addition, it can be expected that the microstructural evolution is essentially resulted from the phase transformations occurring during partial remelting and the study on the phase transformations can offer some important information to further verify the microstructural evolution process.

Therefore, in this work, the microstructural evolution of in-situ Mg_2Si_p/AM60B composite modified by SiC and Sr was investigated during partial remelting, especially the evolution process prior to liquid formation. Simultaneously, the phase transformations occurring during this process and the relations between the phase transformations and microstructural evolution were also discussed.

2 Experimental

The AM60B-based composites reinforced by in-situ Mg_2Si particles in this investigation were prepared by liquid casting method using pure magnesium (99.9%), commercial AM60B magnesium alloy and Al−30%Si (mass fraction). Homemade Mg−30%Sr master alloys and Mg−25%SiC_p press cake (mixture power) were used as grain refiners for Mg_2Si phase and α-Mg phase, respectively. The nominal composition of the AM60B matrix was (5.5%−6.5%) Al, (0.24%−0.6%) Mn, ≤0.22% Zn and ≤0.01% Cu. According to the composition of AM60B−2%Si, all kinds of alloys were melted at 790 °C and held for 30 min, and then modified by 0.5% Sr. After the melt was held for 20 min, 0.2% SiC particles (SiC_p with 7 μm) were introduced and mechanically stirred for 30 s, and then held for 10 min, followed by degassing using C_2Cl_6 and pouring into a permanent mould with ambient temperature to form some rods (d16 mm × 150 mm). The melt was protected by RJ−2 covering agent designed for magnesium alloys during experiment. The casting rods were cut into small specimens (d16 mm × 10 mm). Then, the specimens were heated at a semisolid temperature of 600 °C for different durations and then water-quenched quickly. A hole was drilled along the central axis of a specimen and a thermocouple was mounted in it in order to examine the temperature change of the specimen during partial remelting.

A cross-section (perpendicular to the specimens' axis) of each specimen was processed by standard metallographic techniques, and then observed by scanning electron microscopy (SEM) using back-scattered electron imaging mode and examined by energy disperse spectroscopy (EDS). Subsequently, it was etched by 4% HNO_3 (volume fraction) aqueous solution and observed under an optical microscope. The size and shape factor of primary α-Mg particles in the semisolid microstructures were quantitatively examined using Image-Pro Plus 5.0 software. The details about the examinations can be found in Ref. [29]. On each specimen, three images with magnification of 100 times were examined. X-ray diffractometer (XRD) was employed in order to identify the phase transformations occurring during partial remelting.

3 Results and discussion

3.1 As-cast microstructure

In order to study the microstructural evolution and phase transformations during piratical remelting, the initial as-cast microstructure and solidification process should be clarified at first. Figure 1(a) presents that the primary α-Mg dendrites are fine and equiaxed grains, while Mg_2Si particles are fine and irregular particles. Together with the well-known solidification process of AM60B alloy, it can be suggested that the solidification process of this composite begins with the precipitation of Mg_2Si particles and then the primary α-Mg phases. The first formed Mg_2Si particles are pushed by the growing primary α-Mg phases and distribute in the interdendritic eutectic liquid phase. Finally, the eutectic liquid solidifies into eutectic structures (including eutectic β phase and eutectic Mg_2Si phase), completing the solidification. Therefore, the primary Mg_2Si particles distribute in the interdendritic eutectic structures (Fig. 1(b)). The eutectic α-Mg phase preferentially grows up on the primary α-Mg particles and the eutectic β phases ($Mg_{17}Al_{12}$) are left in the interdendritic regions (Fig. 1(b)).

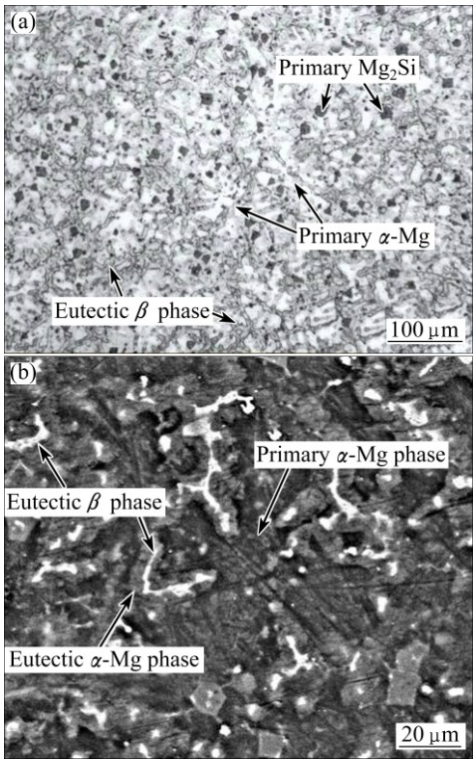

Fig. 1 OM (a) and SEM (b) images of composite treated by 0.5% Sr and 0.2% SiC_p

3.2 Microstructural evolution during partial remelting

Figure 2 shows the microstructures of the modified composite heated for different durations at a semisolid temperature of 600 °C. It can be found that the amount of the eutectic β phase obviously decreases during the period from 0 to 3 min (comparing Fig. 1(b) with Fig. 2(a). The microstructure becomes a grey matrix in which lots of white worm-like and dot-like β phase particles are distributed (Fig. 2(a)). According to the Mg−Al binary phase diagram [30], AM60B alloy will experience a single α-Mg phase interval during heating. So, the β phase dissolves towards the primary α-Mg phase, resulting in the decrease of its amount. Figure 1(b) shows that the β phase in the interdendritic zone is always larger than that between the neighboring dendrite arms in one dendrite. Therefore, it can be expected that the β phases in the interdendritic zone evolve into worm-like morphology and only some dot-like β phases are left in the interdendritic arm regions. It can also be expected that the neighboring dendrite arms within one dendrite will merge when the inter-arm β phase completely dissolves and the neighboring dendrites also possibly merge as the interdendritic β phase completely dissolves in some local zones. Because of composition homogenization occurring during heating, the contrast

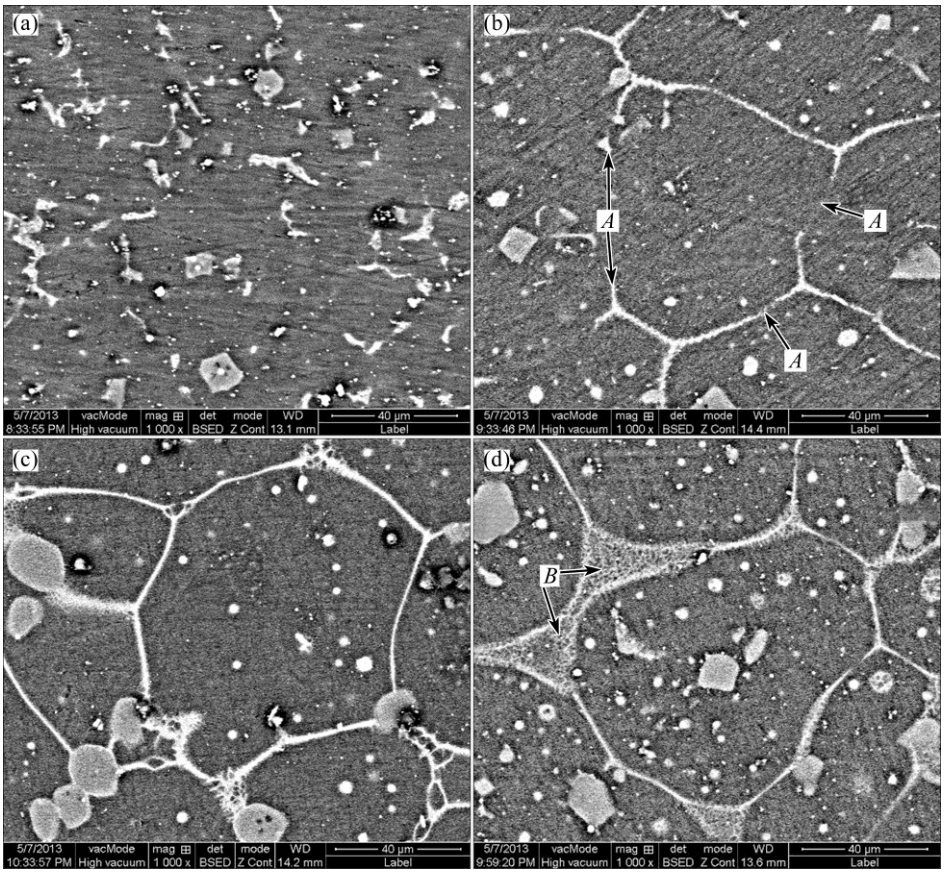

Fig. 2 SEM images of complex modified composites heated at 600 ºC for different durations and then water-quenched: (a) 3 min; (b) 5 min; (c) 7 min; (d) 10 min

difference between the primary α phase and the eutectic α phase decreases. In addition, the gain boundaries also become indistinct due to the dissolution of β phase. It is just because the dendrite morphologies disappear and the matrix evolves into a uniformly grey structure (Fig. 2(a)). It is expected that the original equiaxed dendrites then enter into near spheroidal particles (compact particles without arms) because of the mergence of the neighboring arms (Fig. 2(a)). It should be noted that although the grain boundaries between the dendrites seem to merger together, the actual mergence should be very difficult to occur because the crystal orientations between them should be different. That is to say, the main event occurring during 0−3 min is the rapid coarsening of primary dendrites through mergence of the arms within one dendrite.

As shown in Fig. 3, the heating rate during this stage is very rapid, so there is no enough time for the β phases to completely dissolve (Fig. 2(a)). Some of them are left when the specimen's temperature reaches eutectic point and then melt to form liquid phases (Fig. 3, reaching the eutectic point at 3.6 min). Figure 2(b) shows that the amount of the white structures is larger than that of the residual β phase in Fig. 2(a) and their distribution is also more continuous, which implies that these white structures are not β phase and they should be liquid phase. That is, the residual β phases have melted together with their surrounding α phase at this time. As mentioned above, the neighboring dendrites compactly contact with each other without β phase to separate them, but the energy at the original grain boundaries should be higher than that within the coarsened dendrites due to crystal misorientation [31]. So, it can be suggested that the first formed liquid phase may penetrate along these sites (zones *A* in Fig. 2(b)) or these sites directly melt to form liquid phase as temperature rises. Then, the coarsened dendrites are separated from the neighboring dendrites (Fig. 2(c)). The microstructure evolves into the individually polygonal particles which are separated by thin liquid layers. So, it can be concluded that the structure separation results from the melting of residual eutectic β phase, and the penetration of the first formed liquid along the primary grain boundaries or the grain boundaries melting directly, is the main event during period 3−7 min.

As the heating time is further prolonged, more polygonal particles partially melt due to the temperature rise. Accordingly, the liquid amount increases (comparing Fig. 2(c) with (d)). It is well known that the surface curvature of a crystal has a great effect on its melting point: the larger the curvature is, the lower the melting point is [32]. So, it can be inferred that the edges and corners of the polygonal particles preferentially melt (marked by *B* in Fig. 2(d)), which not only increases the liquid amount, but also leads to the polygonal particles evolving into spheroidal particle (Fig. 4(a)). Figure 4(a) indicates that a semisolid microstructure with small and spheroidal primary particles uniformly suspended in liquid phase is obtained after being heated at 600 °C for 20 min. Therefore, it can be suggested that the main event occurring during period from 7 to 20 min is the spheroidization of the polygonal particles through the melting of their edges and corners.

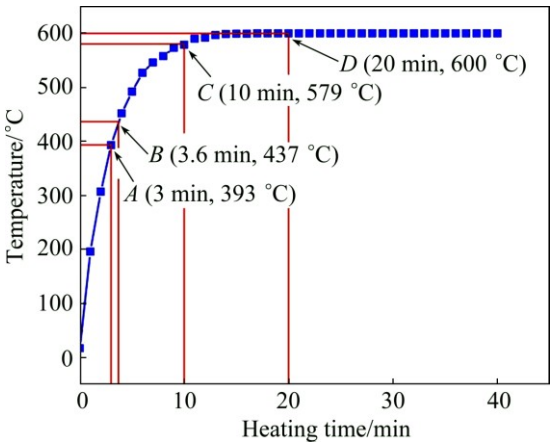

Fig. 3 Variation of temperature in specimen with heating time

Figure 3 shows that the specimen temperature is up to the final value of 600 °C after being heated for 20 min. However, the liquid fraction still increases before 30 min and then basically maintains at about 50% (volume fraction, shown in Fig. 5). Namely, the semisolid system is up to its solid−liquid equilibrium state after being heated for 30 min. It is suggested that the partial remelting of the primary particles during the period from 20 to 30 min still operates although the specimen's temperature reaches the equilibrium value. Figure 4 shows that the main phenomenon occurring during the period from 20 to 30 min is the growth of the primary particles besides the liquid increase. In addition, the semisolid system is not up to the equilibrium state until it is heated for 30 min, namely, the microstructural evolution falls behind the temperature rise.

Figure 4(a) presents that the distance between the neighboring particles is quite short and some particles are only separated by a thin liquid layer. So, it can be expected that the neighboring particles easily contact with each other and mergence may easily operate during the subsequent heating. Figure 4(b) shows that there are some agglomerates composed of two or more particles after the composite being treated for 30 min (marked by arrows). This implies that the coarsening from mergence plays an important role during the period from 20 to 30 min. The driving force of the coarsening is minimizing the solid/liquid interfacial energy through mergence by either grain boundary migration or grain

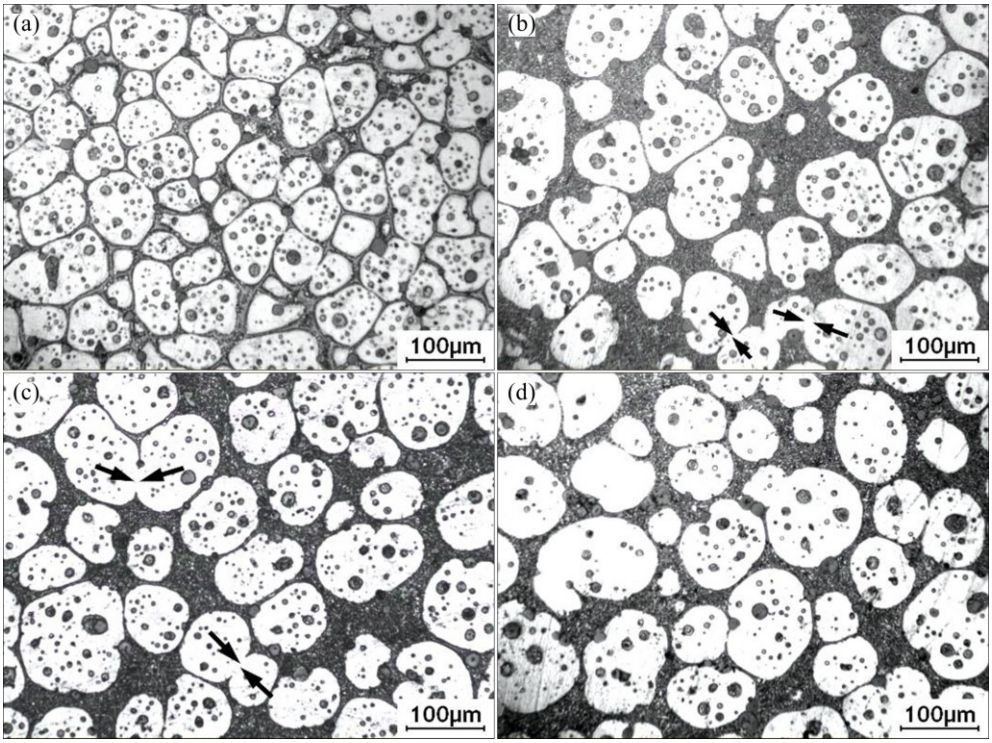

Fig. 4 OM images of complex modified composites heated at 600 °C for different durations and then water-quenched: (a) 20 min; (b) 30 min; (c) 40 min; (d) 60 min

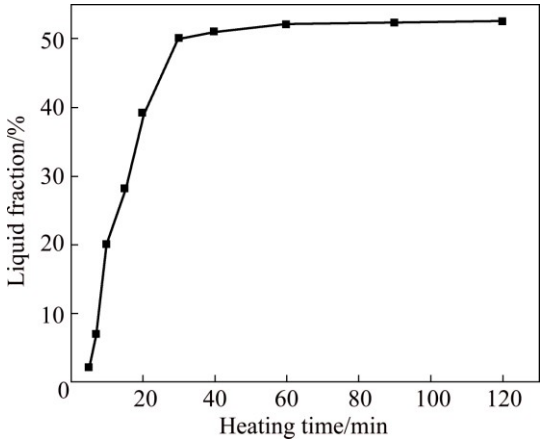

Fig. 5 Variation of liquid fraction of complex modified composites with heating time

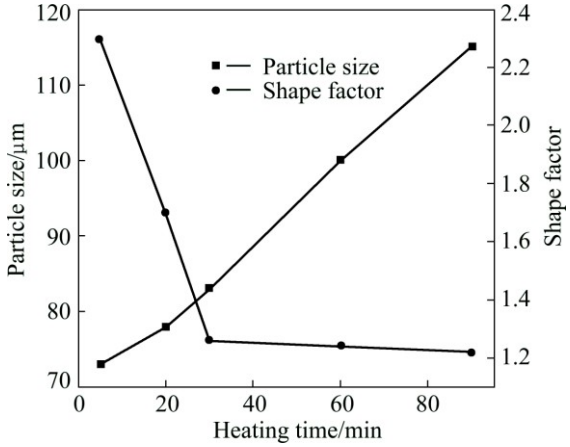

Fig. 6 Variation of primary particle size and shape factor of composite with heating time

rotation (thus minimizing misorientation) [31]. As mentioned above, the liquid fraction still increases from 20 to 30 min and thus the distance between the neighboring particles increases (comparing Figs. 4(a) and (b)). Accordingly, the probability of the merged particles decreases after this period. Figure 6 indicates that the primary particle shape factor slightly decreases after 30 min (comparing the slopes of the corresponding curves). This implies that the particle coarsening regime transfers from a severe regime to a mild regime after 30 min. The Ostwald ripening is a process in which a semisolid system lowers its interfacial energy by reducing its solid/liquid interfacial area through the dissolution of small particles and the growth of large particles [33]. In the Ostwald ripening, the variation of primary particle size obeys the formula, $D^3_t - D^3_0 = Kt$, where D_t is the average particle size at time t, D_0 is the initial particle size and K is the coarsening rate constant [33]. Figure 7 gives the present result, which implies that the coarsening during the period before 30 min does not result from Ostwald ripening, but the coarsening is really attributed to this regime after 30 min. However, it should be mentioned that the coarsening from mergence also operates at the same time, but its effect is relatively small. So, agglomerates are occasionally observed (marked by arrows in Fig. 4(c)).

Furthermore, Ostwald ripening also leads to the dissolution of edges and corners of the particles and the subsequent reprecipitation in sunken zones [33,34], so, the primary particles become more spheroidal and the shape factor decreases (Fig. 4(d) and Fig. 6). It can be concluded that the coarsening after heating for 20 min is resulted from two mechanisms, mergence and Ostwald ripening. The former dominates in the period from 20 to 30 min, while the latter mainly operates after 30 min.

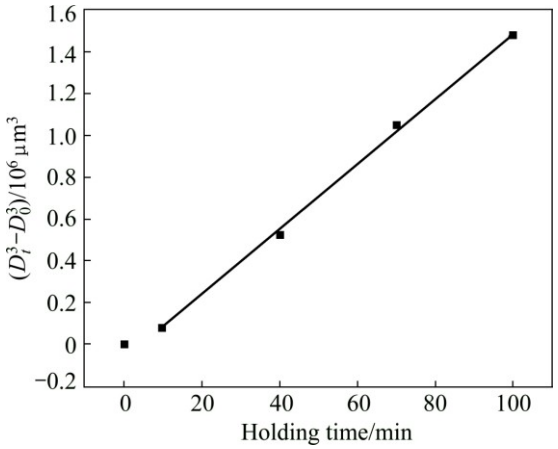

Fig. 7 Cube of primary particle size versus holding time (taking 20 min as starting time, t=0)

Based on the discussion above, it can be concluded that the microstructural evolution during partial remelting includes four steps: the initial rapid coarsening of the dendrites caused by the dissolution of eutectic, the structural separation resulted from the melting of residual eutectic and penetration or melt of the original grain boundaries, the spheroidization of the polygonal particles because the melting of their edges and corners and the final coarsening owing to the mergence and subsequent Ostwald ripening.

3.3 Phase transformations and microstructural evolution mechanisms during partial remelting

As discussed in the above section, the eutectic β phases dissolve towards the primary α phase dendrites, resulting in the decrease in their amount during the initial stage of partial remelting. This is just due to the dissolution that Al content in the primary α phase significantly increases (Table 1) and the corresponding diffraction peaks decrease in the period of 0−3 min (shown in Fig. 8). From the view of phase transformation, the microstructural evolution, i.e., the initial rapid coarsening during the period of 0−3 min is attributed to the reaction of $\beta \rightarrow \alpha$.

As the heating proceeds, the specimen's temperature exceeds the eutectic point, the residual interdendritic β phase then melts to form the liquid phase surrounding the primary particles and the residual inter-arm β phases melt

Table 1 Chemical compositions of different structures of composites heated for different durations at 600 °C and then water-quenched

Heating time/min	Structure	Mass fraction/%	
		Mg	Al
0	Primary α	92.70	7.30
	Eutectic β	77.98	22.02
2.5	Primary α	91.89	8.11
	Eutectic β	83.72	16.28
3	Primary α	91.00	9.00
	Eutectic phase	87.93	12.07
5	Primary α	87.37	12.63
	Liquid phase	90.40	9.60
10	Primary α	85.35	14.65
	Liquid phase	90.73	9.27
20	Primary α	89.67	10.33
	Liquid phase	91.43	8.57
30	Primary α	90.48	9.52
	Liquid phase	91.57	8.43
40	Primary α	90.53	9.47
	Liquid phase	91.64	8.36
60	Primary α	90.48	9.52
	Liquid phase	91.66	8.34
90	Primary α	90.50	9.50
	Liquid phase	91.63	8.37

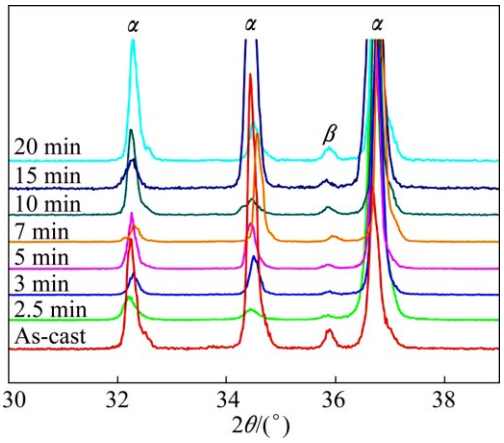

Fig. 8 XRD patterns of composites heated at 600 °C for different time and then water-quenched

to form the liquid pools entrapped within the coarsened dendrites (shown in Fig. 2(b)). The β phase melting can be expressed by the reaction of $\alpha+\beta \rightarrow L$, the reverse eutectic reaction. The first formed liquid phase then penetrates along the original grain boundaries or the grain boundaries directly melt, resulting in the increase of liquid amount (comparing Figs. 2(b) and (c)) and separation of the coarsened dendrites. In view of phase transformation, this penetration or melting can be expressed as the reaction of $\alpha \rightarrow L$. As the Mg-rich α

phase transforms into liquid, the Al content in the liquid phase decreases (Table 1). The liquid solidifies again to form α and β during water-quenching, and the amount of the solidified β phase should increase as the liquid amount increases. So, after heating for 5 min, the diffraction peak intensity of the β phase increases as the time prolongs till the semisolid system up to its equilibrium state (Fig. 8). That is to say, the structural separation is ascribed to the reactions of $\alpha+\beta\rightarrow L$ and $\alpha\rightarrow L$.

After the structure is separated into the individual polygonal particles, the spheroidization operates through melting of the primary α-Mg particles' edges and corners (shown in Fig. 2(d)). From the aspect of phase transformation, the reaction of $\alpha\rightarrow L$ should be responsible for the spheroidization. Due to the melting of α phase, the Al content in the liquid phase further decreases (Table 1). That is to say, the essence of the spheroidization is the partial melting of the primary α phase, i.e., the reaction of $\alpha\rightarrow L$. After being heated for 20 min, the specimen's temperature is up to the final value of 600 °C (point D in Fig. 3). Although the temperature reaches its equilibrium state, the liquid still slightly increases from 20 to 30 min, i.e., the microstructure evolution falls behind the temperature rise. The liquid increase should also be attributed to this reaction.

The semisolid system reaches its final solid−liquid equilibrium state till heating for 30 min. The main phenomenon occurring after 30 min is the coarsening of spheroidal primary particles through Ostwald ripening. Ostwald ripening essentially refers to the dissolution and subsequent reprecipitation. In the view of phase transformation, this process should be $\alpha\rightarrow L$ and $L\rightarrow\alpha$, respectively. During this stage, both the solid and liquid compositions and their amounts do not vary (Fig. 4, Table 1 and Fig. 7).

In fact, Mg_2Si particles also take part in microstructural evolution and phase transformations. However, the solid solubility of silicon atom into α-Mg solid solution is extremely small [30] and the melting point of Mg_2Si particle is relatively high [7]. Therefore, the contribution of Mg_2Si particle in microstructural evolution and phase transformations is a minor influence.

Based on the discussion above, the relationship between the microstructural evolution and phase transformations as discussed above is summarized by Fig. 9. It presents that the initial coarsening results from the reaction of $\beta\rightarrow\alpha$, the structural separation is caused by the reactions of $\alpha+\beta\rightarrow L$ and $\alpha\rightarrow L$, the spheroidization is attributed to the reaction $\alpha\rightarrow L$ and the final coarsening is ascribed to the two reverse reactions of $\alpha\rightarrow L$ and $L\rightarrow\alpha$.

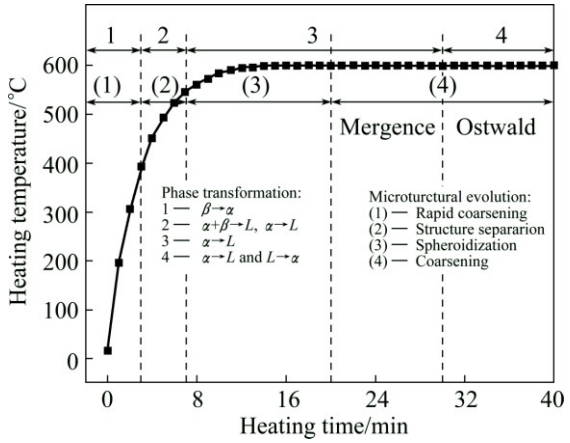

Fig. 9 Illustration of microstructural evolution and phase transformations during partial remelting of complex modified composites at 600 °C

3.4 Effect of Mg_2Si particles on microstructural evolution

The modified Mg_2Si_p/AM60B has a similar microstructural evolution process compared with its matrix alloy, AM60B [21]. However, the microstructural evolution progress of the composite is slower than that of the matrix alloy and the coarsening mechanism is somewhat different. The time for the liquid formation of the matrix alloy is 3 min [21], while that of the composite needs 5 min. The particle coarsening of the composite obeys Ostwald ripening regime after it is heated for 30 min, while that of the matrix alloy does not belong to this regime [21]. For the matrix alloy, the mergence plays an important role in the particle coarsening besides Ostwald ripening. It is known that the conductivity of Mg_2Si particles is smaller than that of the matrix alloy [7] and thus they play an obstruction role in heat transfer. Of course, they also play an obstruction role in mass transfer. So, the microstructural evolution progress of the composite is delayed due to the appearance of Mg_2Si particles. In addition, the pin effect of the Mg_2Si particles in the primary α-Mg boundary prevents the primary α-Mg boundary from rotation or migration [11,35]. Therefore, coarsening through mergence of contacted primary α-Mg particles is suppressed. So, the Ostwald ripening is dominant in the coarsening mechanism. Thus, it can be suggested that the Mg_2Si particles have not obvious effect on the microstructural evolution steps, but influence the evolution progress and coarsening mechanism.

With regard to the morphological evolution of Mg_2Si particles, the related images are shown in Fig. 10. Two kinds of Mg_2Si particles can be observed in the as-cast microstructure: the larger one is primary Mg_2Si particle, and the smaller one is eutectic Mg_2Si particle (Fig. 10(a)). The primary Mg_2Si particles are relatively

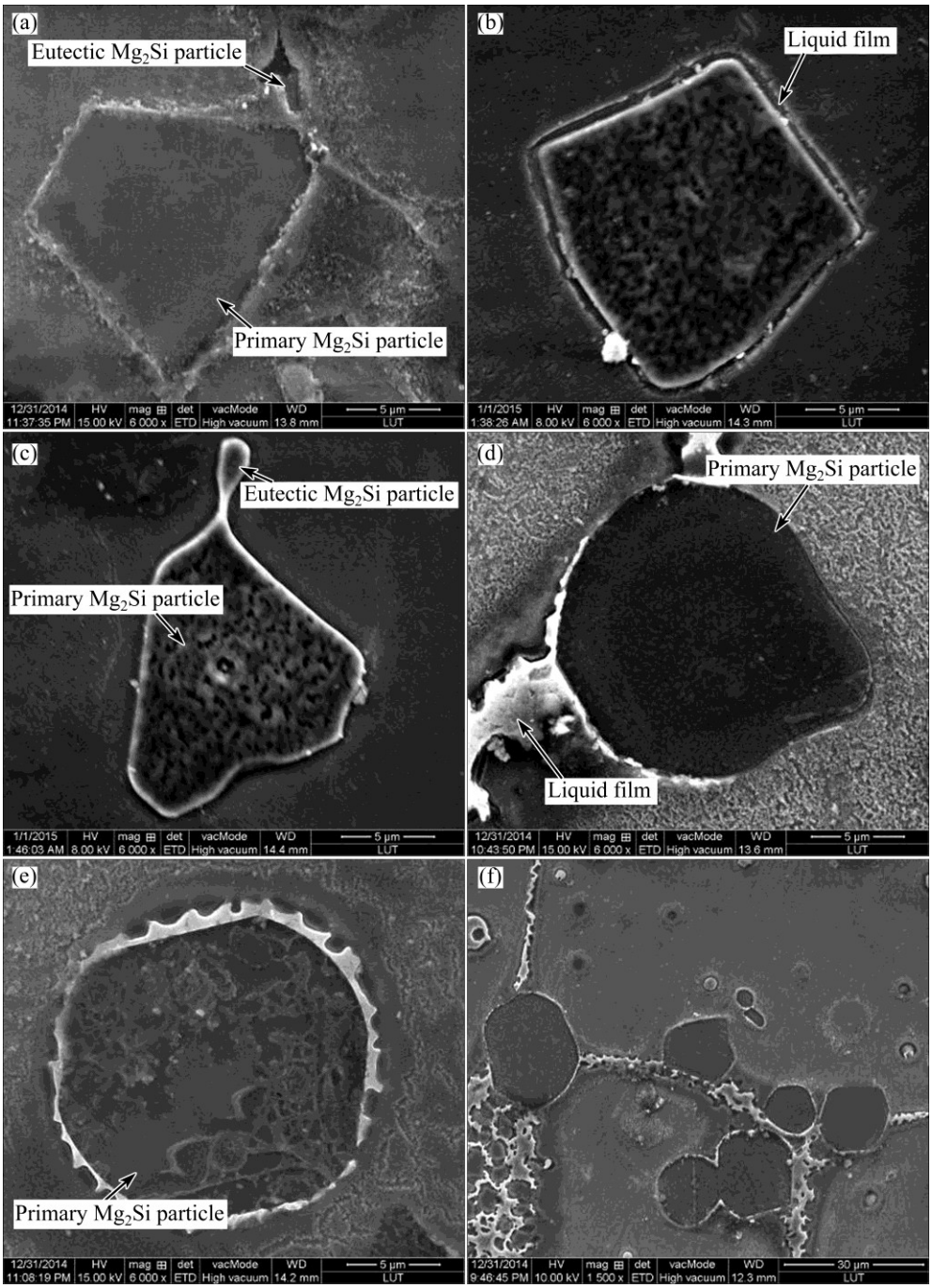

Fig. 10 SEM images of Mg_2Si particles heated for different time: (a) 0 min; (b) 7 min; (c) 10 min; (d) 20 min; (e) 30 min; (f) 60 min

irregular with sharp edges and corners. After being heated for 7 min, the Mg_2Si particles are surrounded by liquid film and their sharp edges and corners tend to become blunt (Fig. 10(b)). The dislocation density surrounding the Mg_2Si particles is larger than that at other sites owing to the mismatch of coefficient of thermal expansion (CTE) between Mg_2Si particles and the matrix [36]. During partial remelting, the matrix surrounding the Mg_2Si particles preferentially melts due to the higher energy at these sites. Although the temperature at this time is lower than the eutectic point of Mg−Mg_2Si alloy (637.6 °C) [30], it can also be expected that the partial melting of Mg_2Si particles occurs at their sharp edges and corners owing to the effect of curvature on melting point. Due to the penetration of the liquid and the melting of the sharp edges and corners, the Mg_2Si particles become blunter and their size decreases (comparing Figs. 10(b) with (c)). Besides this, the eutectic Mg_2Si particles have a tendency to connect with the primary Mg_2Si particles (Fig. 10(c)). As the heating time is prolonged to 20 min, the temperature of the specimen reaches its equilibrium state

(Fig. 3), the Mg_2Si particles evolve into the spheroidal particle and their size is slightly increased (Fig. 10(d)). It can be expected that the melted Mg_2Si particles then reprecipitate in the sunken zones of the primary Mg_2Si particle. Therefore, their morphologies become more and more spheroidal with the extension of heating time. This implies that the coarsening mechanism also obeys Ostwald ripening regime. Ostwald ripening includes the dissolution of small particles and the subsequent reprecipitation on large particles, which results in coarsening and spheroidization of the Mg_2Si particles (Fig. 10(e)). As shown in Fig. 10(f), the Mg_2Si particles cluster is formed after being treated for 60 min. It is expected that the spheroidization is beneficial for taking full reinforcement of Mg_2Si particles while the coarsening and cluster of them should be avoided as possible.

In general, the Mg_2Si particles have not obvious effect on the microstructural evolution steps, but influence the evolution progress and the coarsening mechanism during partial remelting. Their size first decreases due to partial melting and then increases due to Ostwald ripening accompanied by their irregular morphologies evolving from blunt into spheroidal. The coarsening and cluster of them should be avoided as possible.

4 Conclusions

1) A semisolid microstructure with small and spheroidal particles can be obtained after the SiC and Sr modified in-situ Mg_2Si/AM60B composite partially remelted at 600 °C.

2) The microstructural evolution during partial remelting can be divided into four stages, the initial coarsening, structural separation, spheroidization and final coarsening.

3) The microstructural evolution is essentially attributed to the phase transformations occurring during partial remelting. The above four stages are attributed to the phase transformations of $\beta \rightarrow \alpha$, $\alpha+\beta \rightarrow L$ and $\alpha \rightarrow L$, $\alpha \rightarrow L$, and $\alpha \rightarrow L$ and $L \rightarrow \alpha$, respectively.

4) The Mg_2Si particles have not obvious effect on the microstructural evolution steps, but slower the evolution progress. Their morphologies first become blunt and then become spheroidal because of melting of the edges and corners, and finally are coarsened owing to Ostwald ripening.

References

[1] ELIEZER D, AGHION E, FROES F. The science, technology, and applications of magnesium [J]. JOM, 1998, 50(9): 30−34.

[2] LLOYD D J. Particle reinforced aluminium and magnesium matrix composites [J]. International Materials Reviews, 1994, 39(1): 1−23.

[3] EVERETT R K, ARSENAULT R J. Metal matrix composites [M]. San Diego: Academic Press, 1991.

[4] CHEN L, YAO Y. Processing, microstructures, and mechanical properties of magnesium matrix composites: A review [J]. Acta Metallurgica Sinica: English Letters, 2014, 27(5): 762−774.

[5] LI G H, GILL H S, VARIN R A. Magnesium silicide intermetallic alloys [J]. Metallurgical and Materials Transactions A, 1993, 24(11): 2383−2391.

[6] MABUCHI M, HIGASHI K. Strengthening mechanisms of Mg−Si alloys [J]. Acta Mater, 1996, 44(11): 4611−4618.

[7] YU B H, CHEN D, TANG Q B, WANG C L, SHI D H. Structural, electronic, elastic and thermal properties of Mg_2Si [J]. Journal of Physics and Chemistry of Solids, 2010, 71(5): 758−763.

[8] LU Y Z, WANG Q D, ZENG X Q. Effects of silicon on microstructure, fluidity, mechanical properties, and fracture behaviour of Mg−6Al alloy [J]. Materials Science and Technology, 2001, 17(2): 207−214.

[9] MABUCHI M, KUBOTA K, HIGASHI K. Elevated temperature mechanical properties of magnesium alloys containing Mg_2Si [J]. Materials Science and Technology, 1996, 12(1): 35−39.

[10] SHEN Le, CHEN Ti-jun, MA Ying, LIU Ming-wei, HAO Yuan. Modification of in-situ Mg_2Si/AM60B magnesium matrix composites with $MgCO_3$ and Sr [J]. Special Casting and Nonferrous Alloys, 2011, 31(7): 653−655. (in Chinese)

[11] HONG T W, KIM S K, HA H S, KIM M G, LEE D B, KIM Y J. Microstructural evolution and semisolid forming of SiC particulate reinforced AZ91HP magnesium composites [J]. Materials Science and Technology, 2000, 16(7): 887−892.

[12] JI S, QIAN M, FAN Z. Semisolid processing characteristics of AM Series Mg aloys by rheo-diecasting [J]. Metallurgical and Materials Transactions A, 2006, 37(3): 779−787.

[13] KIRKWOOD D H. Semisolid metal processing [J]. International Materials Reviews, 1994, 39(5): 173−189.

[14] FLEMINGS M C. Behavior of metal alloys in the semisolid state [J]. Metallurgical and Materials Transactions A, 1991, 22(5): 957−981.

[15] LIU D, ATKINSON H V, KAPRANOS P, JIRATTITICHAROEAN W, JONES H. Microstructural evolution and tensile mechanical properties of thixoformed high performance aluminium alloys [J]. Materials Science and Engineering A, 2003, 361(1−2): 213−224.

[16] XIA K, TAUSIG G. Liquidus casting of a wrought aluminum alloy 2618 for thixoforming [J]. Materials Science and Engineering A, 1998, 246(1): 1−10.

[17] GUO Ming-hai, LIU Jun-you, LI Yan-xia. Microstructure and properties of SiC_p/Al electronic packaging shell produced by liquid–solid separation [J]. Transactions of Nonferrous Metals Society of China, 2014, 24(4): 1039−1045.

[18] JIA Qin-jin, LIU Jun-you, LI Yan-xia, WANG Wen-shao. Microstructure and properties of electronic packaging box with high silicon aluminum-base alloy by semi-solid thixoforming [J]. Transactions of Nonferrous Metals Society of China, 2013, 23(1): 80−85.

[19] CHEN Ti-jun, MA Ying, WANG Rui-quan, LI Yuan-dong, HAO Yuan. Microstructural evolution during partial remelting of AM60B magnesium alloy refined by $MgCO_3$ [J]. Transactions of Nonferrous Metals Society of China, 2010, 20(9): 1615−1621.

[20] JIANG Ju-fu, WANG Ying, QU Jian-jun, DU Zhi-ming, LUO Shou-jing. Preparation and thixoforging of semisolid billet of AZ80 magnesium alloy [J]. Transactions of Nonferrous Metals Society of China, 2010, 20(9): 1731−1736.

[21] CHEN Ti-jun, LÜ Wei-bin, MA Ying, HUANG Hai-jun, HAO Yuan. Semisolid microstructure of AM60B magnesium alloy refined by SiC particles [J]. International Journal of Materials Research, 2011, 102(12): 1459−1467.

[22] FAN Z. Semisolid metal processing [J]. International Materials Reviews, 2002, 47(2): 49−85.
[23] FAN Z, CHEN J Y. Modelling of rheological behaviour of semisolid metal slurries [J]. Materials Science and Technology, 2002, 18(3): 243−249.
[24] JIANG Ju-fu, WANG Ying, LIU Jun, QU Jian-jun, DU Zhi-ming, LUO Shou-jung. Microstructure and mechanical properties of AZ61 magnesium alloy parts achieved by thixo-extruding semisolid billets prepared by new SIMA [J]. Transactions of Nonferrous Metals Society of China, 2013, 23(3): 576−585.
[25] XING Bo, HAO Yuan, LI Yuan-dong, MA Ying, CHEN Ti-jun. Microstructure control of AZ31 alloy by self-inoculation method for semisolid rheocasting [J]. Transactions of Nonferrous Metals Society of China, 2013, 23(3): 567−575.
[26] YAO J, SUN Z, YANG T, BBUSHAN B, LONG W, ZHANG L. Microstructure and property of rheocasting AZ91 slurry produced via ultrasonic vibration process [J]. Transactions of Nonferrous Metals Society of China, 2014, 23(3): 619−625.
[27] STJOHN D H, QIAN M, EASTON M A, CAO P, HILDEBRAND Z. Grain refinement of magnesium alloys [J]. Metallurgical and Materials Transactions A, 2005, 36(7): 1669−1679.
[28] ZHA M, WANG H Y, XUE P F. Microstructural evolution of Mg−5Si−lAl alloy during partial remelting [J]. Journal of Alloys and Compounds, 2009, 472(1−2): 18−22.
[29] CHEN T J, HAO Y, LI Y D, MA Y. Effect of solid solution treatment on semisolid microstructure of dendritic zinc alloy ZA27 [J]. Materials Science and Technology, 2008, 24(11): 1313−1320.
[30] MASSALSKI T B, OKAMOTO H. Binary alloys phase diagrams [M]. Ohio: ASM International, 1990.
[31] TZIMAS E, ZAVALIANGOS A. Evolution of near-equiaxed microstructure in the semisolid state [J]. Materials Science and Engineering A, 2000, 289(1): 228−240.
[32] CHEN P C, ZHU L M, LI Z. Fundamental of metal forming [M]. Beijing: China Machine Press, 2003. (in Chinese)
[33] SNYDER V A, ALKEMPER J, VOORHEES P W. The development of spatial correlations during Ostwald ripening: A test of theory [J]. Acta Mater, 2000, 48(10): 2689−2701.
[34] LUO S J, CHEN Q, ZHAO Z D. An investigation of microstructure evolution of RAP processed ZK60 magnesium alloy [J]. Materials Science and Engineering A, 2009, 501(1−2): 146−152.
[35] CZERWINSKI F, ZIELINSKA-LIPIEC A. The microstructure evolution during semisolid molding of a creep-resistant Mg−5Al−2Sr alloy [J]. Acta Mater, 2005, 53(12): 3433−3444.
[36] ARSENAULT R J, SHI N. Dislocation generation due to differences between the coefficients of thermal expansion [J]. Materials Science and Engineering A, 1986, 81: 175−187.

原位 Mg_2Si_p/AM60B 复合材料在部分重熔过程中的组织演变和相变

张素卿，陈体军，程发良，李雷亮

兰州理工大学 省部共建有色金属先进加工与再利用国家重点实验室，兰州 730050

摘 要：研究由 SiC 和 Sr 改性的原位 Mg_2Si_p/AM60B 复合材料在部分重熔过程中的组织演变和相变。结果表明：SiC 和 Sr 可以有效地细化初生 α-Mg 晶粒和 Mg_2Si 颗粒。部分重熔以后，可以获得具有细小球状初始 α-Mg 颗粒的半固态组织。部分重熔过程中的组织演变可以分为 4 个阶段：快速粗化、组织分离、球状化和最终的粗化。组织演变的实质是因为发生相变：$\beta\rightarrow\alpha$，$\alpha+\beta\rightarrow L$ 和 $\alpha\rightarrow L$，$\alpha\rightarrow L$，$\alpha\rightarrow L$ 和 $L\rightarrow\alpha$。Mg_2Si 颗粒对于组织演变步骤没有太大影响，但会减慢演变进程且改变粗化机制。复合材料部分重熔时，由于 Mg_2Si 颗粒的边角优先熔化，颗粒首先变钝，然后呈球状化，最后在 Ostwald 熟化作用下粗化。

关键词：镁合金；部分重熔；触变成形；组织演变；相转变；原位复合材料

(Edited by Wei-ping CHEN)